Progress In Electromagnetics Research Letters, Vol. 59, 63–69, 2016

Mutual Coupling Reduction between Printed Dual-Frequency Antenna Arrays

Lin Li[1, 2], Yantao Yu[2, *], and Lijun Yi[2]

Abstract—A new defected ground structure (DGS) is designed to reduce the mutual coupling of a dual-frequency printed monopole array. The designed dual-frequency DGS consists of two concentric split ring slots. Each split ring slot produces band rejection characteristics at one resonant frequency of the antennas. An effective equivalent circuit model of the DGS section is proposed with the circuit parameters successfully extracted. Good agreement exists among the circuit simulation, EM simulation and experimental results. With the inclusion of the DGS, the measured mutual coupling of the dual-band array has been effectively reduced by 10 dB and 20 dB at two resonant frequencies, respectively.

1. INTRODUCTION

A multi-port antenna array has become a crucial part in new generation of wireless communication systems because it can provide higher data rates and increase system capacity by adding extra information channels. However, the space for multiple antennas in a mobile device is usually very limited, which results in a compact antenna array. The mutual coupling effect between closely spaced array elements becomes severe and may dramatically degrade the radiation characteristics of the antenna system. Various techniques to reduce the mutual coupling of antenna arrays have been reported. The decoupling networks using reactive components [1], microstrip sections [2] or hybrid couplers [3, 4] can be added to the feeding ports of the array to reduce mutual coupling. In signal processing, the coupling matrices using receiving mutual impedance [5–7] can be applied to compensate for the mutual coupling in the received signal vectors. For printed antennas, electromagnetic band-gap (EBG) structures using the mushroom-like topology [8] can be used, but the involving of vias increases the circuit complexity and design cost. Defected ground structures (DGS) are widely used in microwave circuit and antenna design due to its band rejection characteristics similar to EBG structures but with a more compact size [9–11]. However, most of the work is for arrays with single operating frequency. While with the rapid development of wireless communications, dual-band or multi-band antennas are increasingly demanded. A dual-band decoupling network using synthesized microstrip lines is described in [12]. The port isolation of dual-frequency array for mobile terminals has been enhanced by implementing a defected ground structure and microstrip matching network [13]. However, these designs are a bit complicated.

In this paper, mutual coupling reduction in a printed dual-frequency monopole array using simple defected ground structures is presented. The proposed dual-frequency DGS consists of two concentric split ring slots. An effective equivalent circuit model of the DGS section is proposed. The theory is validated by measurements on fabricated prototypes.

Received 6 February 2014, Accepted 21 March 2016, Scheduled 3 April 2016

* Corresponding author: Yantao Yu (yantaoyu@cqu.edu.cn).

[1] Chongqing College of Electronic Engineering, Chongqing 401331, China. [2] College of Communication Engineering, Chongqing University, Chongqing 400044, China.

2. CHARACTERISTICS OF DUAL-BAND DGS

2.1. Design of the Dual-Band DGS

Figure 1 shows a typical planar microstrip structure with the proposed DGS. The white concentric split ring slots represent the defects and are etched off the ground plane, which is the dark region in the schematic diagram. A pair of dashed lines represents a microstrip line on the reverse side of the substrate. An FR4 substrate with a relative permittivity ε_r of 4.4, thickness of 1.6 mm and loss tangent of 0.02 is used for all the designs in this paper. The 50 Ω microstrip line has a width of $W_0 = 3$ mm. In order to investigate its frequency characteristics, the DGS section is simulated by using the EM simulator, Ansoft HFSS. Figures 2 and 3 show the simulated S_{21} for different r_1 and r_3, where r_1 is the outer radius of the larger split ring slot and r_3 the outer radius of the smaller one, respectively. The simulation results show that the proposed DGS has two stop bands. As r_1 increases, the lower stop band frequency decreases while the upper stop band frequency remains stable. Similarly, the variation of r_3 mostly affects the upper stop band frequency. It is observed that the larger the center radius of the split ring slot, the lower the corresponding stop band frequency. That is, the length of the split ring slot plays the most important role in determining its resonant frequency. By properly tuning the dimensions of the DGS section, the desired band rejection characteristics can be achieved.

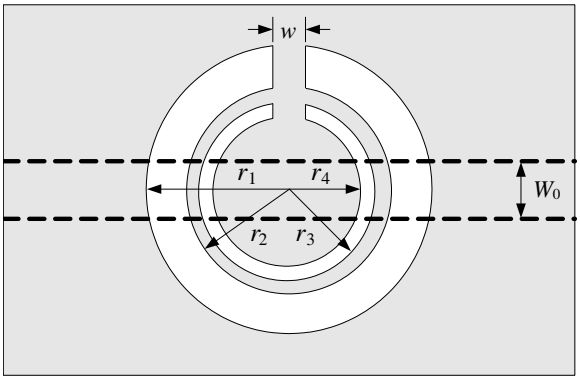

Figure 1. The proposed DGS etched in the ground plane of a microstrip line.

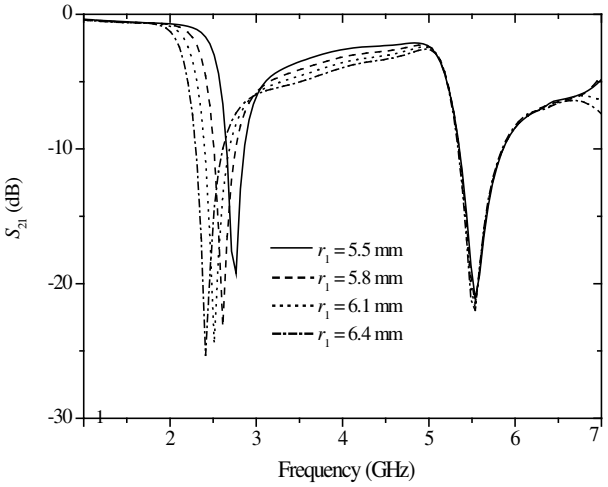

Figure 2. The transmission coefficient of the DGS section with variation of r_1.

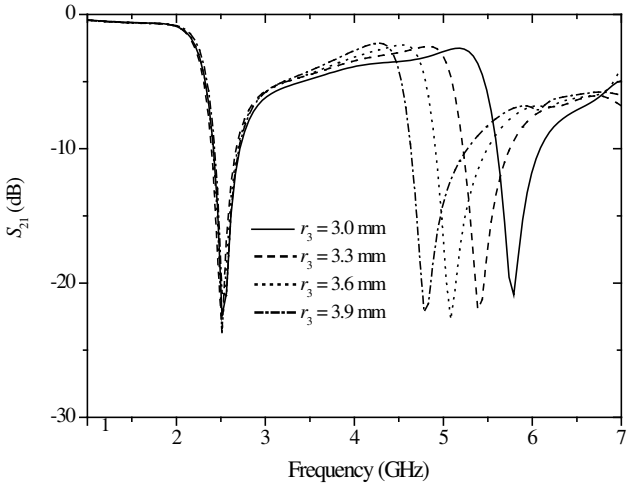

Figure 3. The transmission coefficient of the DGS section with variation of r_3.

2.2. Circuit Model of the Dual-Band DGS

To get a clear insight into the coupling mechanism between the microstrip line and DGS section, a simple and accurate equivalent circuit model for the proposed DGS section is derived.

The coupling between the microstrip line and each slot is due to magnetic field coupling and can be modeled by an ideal transformer with a turn ratio given by [14]

$$n = \sqrt{\frac{Z_{in}}{Z_L}} \cong \sqrt{\frac{Z_0^{strip}}{Z_0^{slot}}}, \tag{1}$$

where Z_0^{strip} and Z_0^{slot} are the characteristic impedances of the microstrip line and the slot line, respectively and can be easily determined by [15]. Since the performance of the DGS seems like two one-pole bandstop filters operating at two different frequencies, the parallel equivalent circuit shown in Figure 4 can be used to model the proposed DGS section. For a more accurate and reliable model, a lossy characteristics of the coupling of microstrip line and DGS is considered. Instead of using the prototype low-pass filter characteristics in [16], the equivalent parameters in the circuit model are extracted from the physical structure. Firstly, the input admittance of the slot, Y_{in}^{slot}, is determined by [17]

$$Y_{in}^{slot} = \left(Z_0^{slot} \cdot \frac{1 - j \tanh \alpha l \cot \beta l}{\tanh \alpha l - j \cot \beta l} \right)^{-1} \tag{2}$$

where α is the attenuation constant and β the phase constant, which can be calculated according to the microstrip line theory, and l is the electrical resonant length of the slot [18]. Y_{in}^{slot} can be seen as a load of microstrip line, Y_L and then following the procedures in [19], the resistance, capacitance and inductance in the equivalent circuit can be obtained by

$$R = 1/\mathrm{Re}\left(\frac{Y_{in}^{slot}}{n^2} \right) \tag{3}$$

$$C = \frac{\mathrm{Im}\left(\frac{Y_{in}^{slot}}{n^2} \right)}{2\pi f_0 (f_0/f_c - f_c/f_0)} \tag{4}$$

$$L = \frac{1}{4\pi^2 f_0^2 C} \tag{5}$$

where f_0 is the frequency of the attenuation pole location and f_c the 3 dB cut-off frequency of a band-reject response.

In order to verify the validity of this equivalent circuit, a sample of the DGS section in Figure 1 with parameters of $r_1 = 6.1\,\mathrm{mm}$, $r_2 = 5.2\,\mathrm{mm}$, $r_3 = 3.2\,\mathrm{mm}$, $r_4 = 2.5\,\mathrm{mm}$ and $w = 2\,\mathrm{mm}$ was studied, and the fabricated prototype is shown in Figure 5. It can be seen from Figure 6 that two stop bands appear at 2.1 GHz and 5.4 GHz with attenuation levels of $-29\,\mathrm{dB}$ and $-23\,\mathrm{dB}$, respectively. The circuit parameters extracted from the simulated S-parameters are $R_1 = 1.104\,\mathrm{k\Omega}$, $C_1 = 1.912\,\mathrm{pF}$, $L_1 = 3.007\,\mathrm{nH}$, $R_2 = 1.058\,\mathrm{k\Omega}$, $C_2 = 1.3\,\mathrm{pF}$, and $L_2 = 0.67\,\mathrm{nH}$. The results among the equivalent circuit analysis, the full wave EM simulation and measurement are compared and demonstrated in Figure 6. As shown in the figure, the result obtained from the proposed equivalent circuit analysis has a good agreement with that from the EM simulation and measurement. In addition, the result from the equivalent circuit analysis using the prototype low-pass filter characteristics (LPF) is also shown in Figure 6 for comparison. It is obvious that the proposed equivalent circuit model has better approximation to the EM simulation than that based on the prototype low-pass filter.

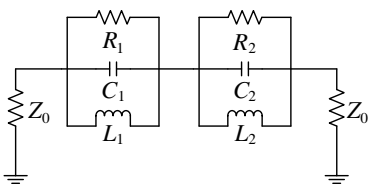

Figure 4. The equivalent circuit model of the DGS section under a microstrip line.

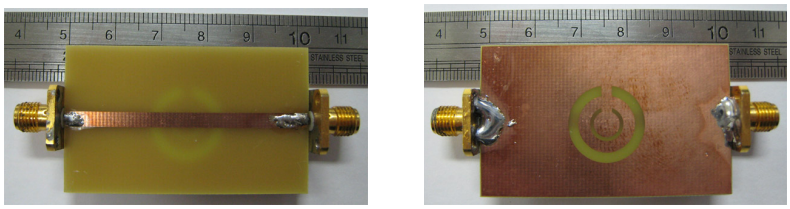

(a) (b)

Figure 5. The fabricated prototype of the DGS section. (a) Top view; (b) bottom view.

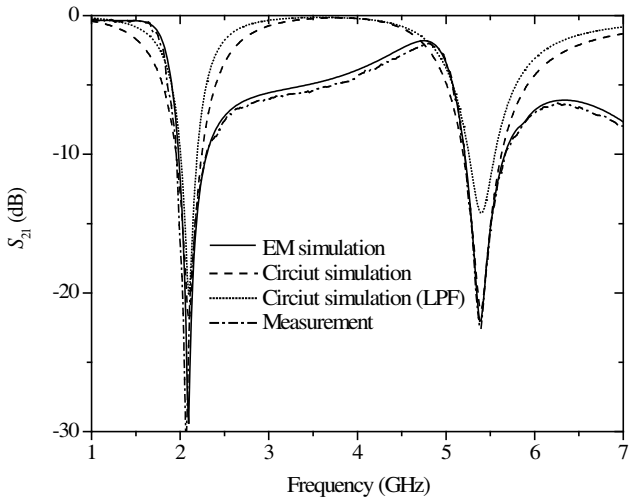

Figure 6. Frequency response of theoretical analysis (proposed circuit model and LPF circuit model), EM simulation, and measurement.

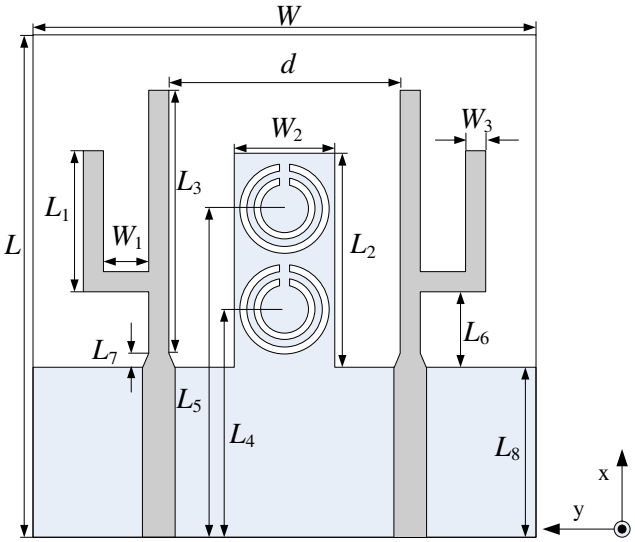

Figure 7. The structure of the printed monopole array with DGS.

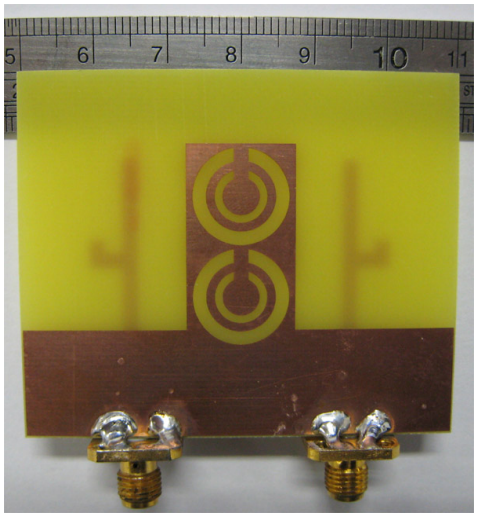

Figure 8. The back view of the fabricated printed array with DGS.

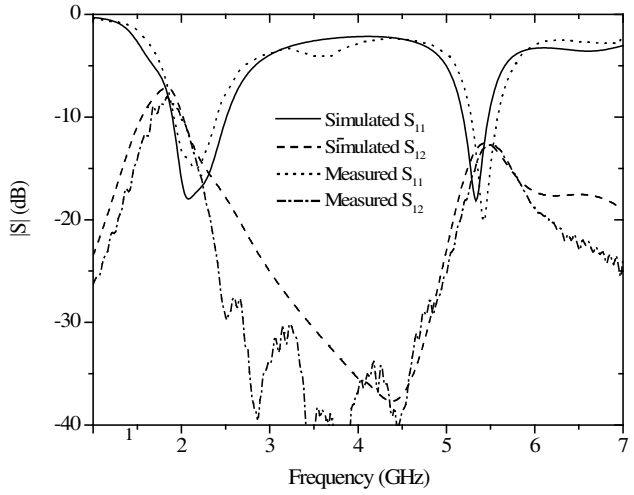

Figure 9. The S-parameters of the printed monopole array without DGS.

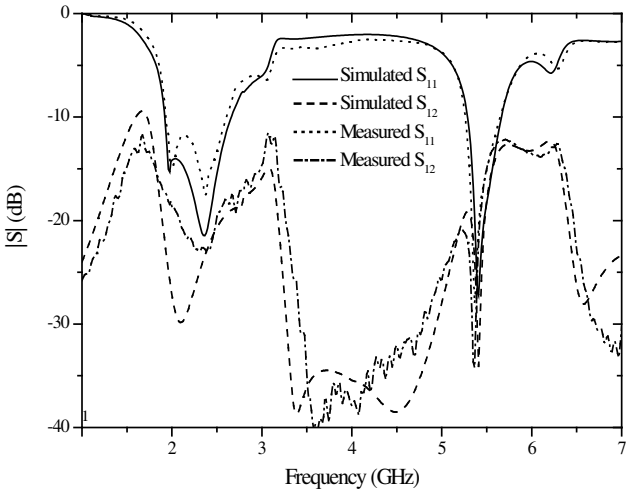

Figure 10. The S-parameters of the printed monopole array with DGS.

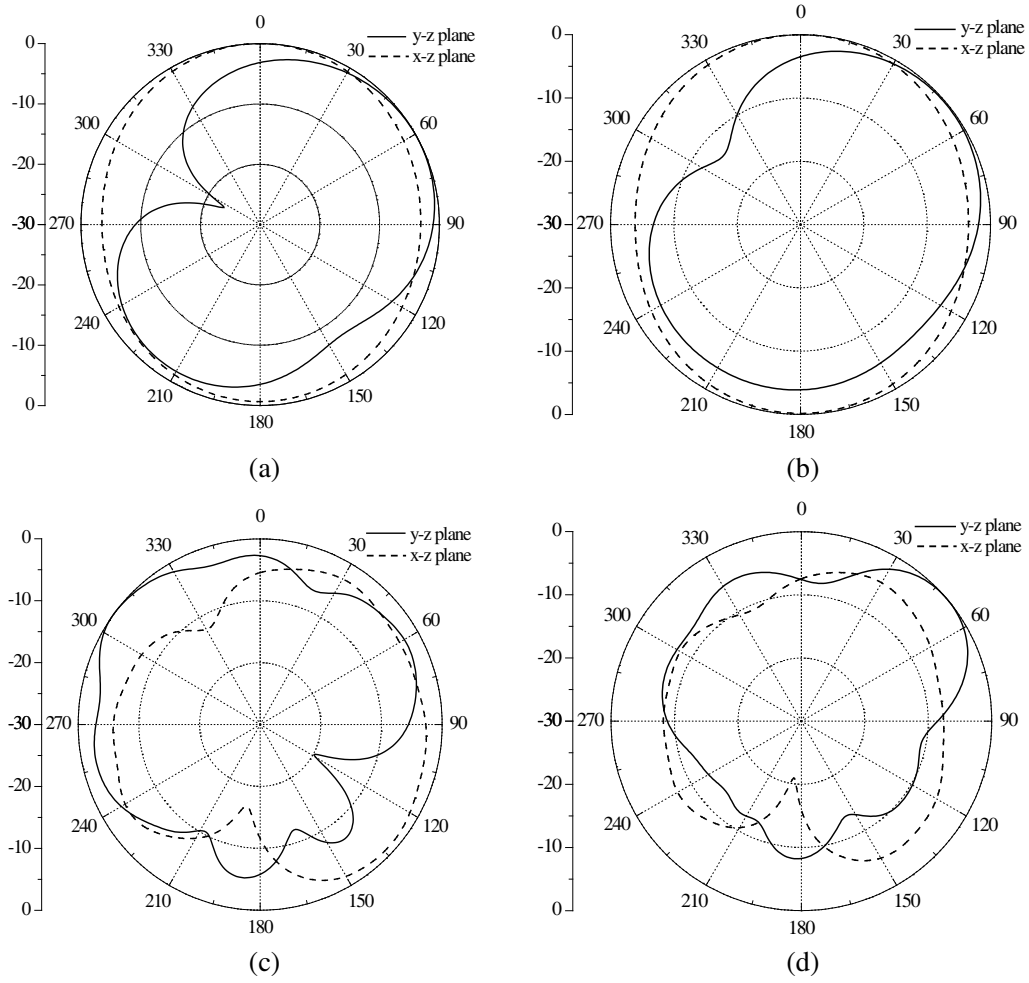

Figure 11. Normalized radiation patterns. (a) 2.1 GHz w/o DGS; (b) 2.1 GHz with DGS; (c) 5.4 GHz w/o DGS; (d) 5.4 GHz with DGS.

3. MUTUAL COUPLING REDUCTION

The strong dual-band rejection characteristics observed for the concentric split ring slot DGS may be exploited to reduce the mutual coupling of a compact dual-band antenna array. As an illustration, a two-element 4-shaped dual-band monopole antenna array operating at 2.1 GHz and 5.4 GHz is designed, as shown in Figure 7 and Figure 8. The dimensions of the antennas are $W = 60\,\text{mm}$, $L = 50\,\text{mm}$, $W_1 = 2.7\,\text{mm}$, $L_1 = 3.3\,\text{mm}$, $W_2 = 14.7\,\text{mm}$, $L_2 = 25\,\text{mm}$, $W_3 = 2\,\text{mm}$, $L_3 = 23\,\text{mm}$, $L_4 = 19.5\,\text{mm}$, $L_5 = 33\,\text{mm}$, $L_6 = 9\,\text{mm}$, $L_7 = 1.67\,\text{mm}$, $L_8 = 15\,\text{mm}$ and the distance between the antennas is $d = 28\,\text{mm}$. The monopole array is printed on the same FR4 substrate used in the DGS section. As shown in Figure 7, two units of the proposed DGS section are etched out from the extended ground plane of the array. This configuration ensures the effective minimization of the mutual coupling between the elements. The transmission coefficient between the two printed monopoles is determined to gauge the mutual coupling effect.

Figures 9 and 10 show the simulated and measured S-parameters of the dual-frequency monopole array with and without the DGS inclusions, respectively. It can be seen that the measured results agree well with the simulated ones. Without the inclusion of DGS, the coupling coefficient of the array is about $-12.2\,\text{dB}$ at 2.1 GHz and $-12.6\,\text{dB}$ at 5.4 GHz. With the DGS etched out of the ground plane, the reduction of about 10 dB at 2.1 GHz and more than 20 dB at 5.4 GHz in the mutual coupling between the antennas is observed. The high port isolation of the monopole array makes it suitable for multiple antenna communications. The radiation patterns of the array were computed by exciting one of the antennas and loading the other with a $50\,\Omega$ impedance. It is shown in Figure 11 that the radiation patterns of the monopole array remain their general shapes before and after implementing the DGS at both resonant frequencies, respectively. However, there are minor variations in the patterns mainly existing in the lower semisphere due to the increased backward radiation.

4. CONCLUSION

The mutual coupling reduction of a printed dual-band monopole array by using compact DGS has been described. The effective equivalent circuit model of the DGS section provides a physical understanding of the problem of the DGS. Good agreement has been achieved among the circuit simulation, EM simulation and experimental results. With the inclusion of the DGS, the mutual coupling of the array has been effectively reduced at two resonant frequencies. Increased port isolation makes the array suitable for applications in multi-antenna wireless communications.

ACKNOWLEDGMENT

This work was supported in parts by the National Natural Science Foundation of China (grant 61101024), the open research fund of Chongqing Key Laboratory of Emergency Communications and the Fundamental Research Funds for the Central Universities (grant 106112014CDJZR165504).

REFERENCES

1. Dossche, S., S. Blanch, and J. Romeu, "Optimum antenna matching to minimize signals correlation on a two-port antenna diversity system," *Electronics Lett.*, Vol. 40, No. 19, 1164–1165, 2004.
2. Hong, T. and Y. Yu, "A compact monopole array with increased port isolation," *Journal of Electromagnetic Waves and Applications*, Vol. 25, No. 8/9, 1213–1220, 2011.
3. Lee, T.-I. and Y. Wang, "Mode-based information channels in closely coupled dipole pairs," *IEEE Trans. Antennas Propag.*, Vol. 56, No. 12, 3804–3811, 2008.
4. Coetzee, J. C. and Y. Yu, "Port decoupling for small arrays by means of an eigenmode feed network," *IEEE Trans. Antennas Propag.*, Vol. 56, No. 6, 1587–1593, 2008.
5. Lui, H.-S. and H. T. Hui, "Effective mutual coupling compensation for direction-of-arrival estimations using a new, accurate determination method for the receiving mutual impedance," *Journal of Electromagnetic Waves and Applications*, Vol. 24, No. 2/3, 271–281, 2010.

6. Lui, H. S. and H. T. Hui, "Mutual coupling compensation for direction-of-arrival estimations using the receiving-mutual-impedance method," *International Journal of Antennas and Propagation*, March 2010.
7. Lui, H.-S., H. T. Hui, and M. S. Leong, "A note on the mutual coupling problems in transmitting and receiving antenna array," *IEEE Antennas and Propagations Magazine*, Vol. 51, No. 5, 171–176, 2009.
8. Yang, F. and Y. Rahmat-Samii, "Microstrip antennas integrated with electromagnetic band-gap (EBG) structures: a low mutual coupling design for array applications," *IEEE Trans. Antennas Propag.*, Vol. 51, No. 10, 2936–2946, 2003.
9. Kim, C.-S., J.-S. Lim, S. Nam, K.-Y. Kang, and D. Ahn, "Equivalent circuit modeling of spiral defected ground structure for microstrip line," *Electron. Lett.*, Vol. 38, 1109–1111, 2002.
10. Jiang, Y., Y. Yu, M. Yuan, and L. Wu, "A compact printed monopole array with defected ground structure to reduce the mutual coupling," *Journal of Electromagnetic Waves and Applications*, Vol. 25, No. 14/15, 1963–1974, 2011.
11. Bait-Suwailam, M. M., O. F. Siddiqui, and O. M. Ramahi, "Mutual coupling reduction between microstrip patch antennas using slotted-complementary split-ring resonators," *IEEE Antennas Wireless Propag. Lett.*, Vol. 9, 876–878, 2010.
12. Lin, K.-C., C.-H. Wu, C.-H. Lai, and T.-G. Ma, "Novel dual-band decoupling network for two-element closely spaced array using synthesized microstrip lines," *IEEE Trans. Antennas Propag.*, Vol. 60, No. 11, 5118–5128, 2012.
13. Sharawi, M. S., A. B. Numan, M. U. Khan, and D. N. Aloi, "A dual-element dual-band MIMO antenna system with enhanced isolation for mobile terminals," *IEEE Antennas Wireless Propag. Lett.*, Vol. 11, 1006–1009, 2012.
14. Caloz, C., H. Okabe, T. Iwai, and T. Itoh, "A simple and accurate model for microstrip structures with slotted ground plane," *IEEE Microwave and Wireless Components Letters*, Vol. 14, No. 3, 127–129, 2004.
15. Gupta, K. C., R. Garg, I. Bahl, and P. Bhartia, *Microstrip lines and Slotlines*, 2nd Edition, Artech House, Norwood, NJ, 1996.
16. Ahn, D., J.-S. Park, C.-S. Kim, J. Kim, Y. Qian, and T. Itoh, "A design of the low-pass filter using the novel microstrip defected ground structure," *IEEE Trans. Microwave Theory Techniques*, Vol. 49, No. 1, 86–93, 2001.
17. Pozar, D. M., *Microwave Engineering*, 3rd Edition, Wiley, Hoboken, NJ, 2005.
18. Axelrod, A., M. Kisliuk, and J. Maoz, "Broadband microstip-fed slot radiator," *Microwave Journal*, Vol. 32, 81–94, 1989.
19. Wu, H.-W., M.-H. Weng, Y.-K. Su, R.-Y. Yang, and C.-S. Ye, "An effective equivalent circuit model of slotted ground structures under planar microstrip," *Microwave and Optical Technology Letters*, Vol. 50, No. 10, 2651–2653, 2008.